

ESSnuSB LINAC AND TRANSFER LINE: LATTICE DESIGN AND ERROR STUDIES

N. Blaskovic Kraljevic*, M. Eshraqi, B. T. Folsom, ESS, Lund, Sweden

Abstract

The ESS neutrino superbeam (ESSnuSB) project is being studied as an upgrade to the European Spallation Source (ESS). This proposed upgrade consists of adding an H^- source to the existing beamline in order to send H^- pulses in between proton pulses, effectively doubling the beam power from 5 MW to 10 MW. In this contribution, we present the 2.5 GeV linear accelerator (linac) lattice and the design of the transfer line from the linac to the accumulator ring, where pulses would be stacked to achieve short proton pulses of high intensity. The results of error studies, quantifying the effect of accelerator imperfections and H^- ion stripping losses on the beam transport through the linac and transfer line, are also presented.

INTRODUCTION

The ESS neutrino superbeam (ESSnuSB) project [1,2] is a design to make use of the European Spallation Source (ESS) linac [3,4] for neutrino production. This project requires interleaving the 5 MW ESS proton beam with an additional 5 MW H^- ion beam, then diverting the H^- beam at the end of the ESS linac through a linac-to-ring (L2R) transfer line for injection by charge exchange injection into an accumulator ring. The resulting proton pulses are stacked in the ring in order to produce short proton pulses (~ 1 ms) of high intensity. The accumulated pulses are then extracted through a switchyard to a target to produce pions which are focused by four magnetic horns. This is followed by a beam dump and an onsite near neutrino detector. The ESSnuSB layout is shown in Fig. 1. A far detector would then be located at a distance of around 500 km, allowing for a high-sensitivity study of the neutrino mixing angle at the second oscillation peak [5].

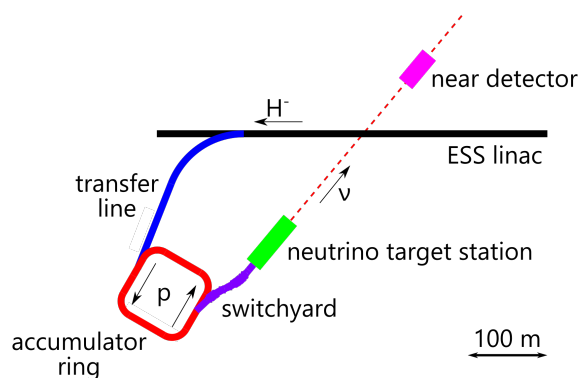


Figure 1: Overview of the ESSnuSB layout [6].

* neven.blaskovickraljevic@ess.eu

LINAC AND L2R DESIGN

The design of the ESS linac currently under construction in Lund, Sweden, is shown in Fig. 2. The ESSnuSB upgrade involves increasing the final energy from 2 GeV to 2.5 GeV by increasing the length of the High- β Line (HBL) by around 70 m. It is at the end of this upgraded HBL that the L2R line starts, bending the beam both horizontally away from the linac and vertically down towards the underground accumulator ring as shown in the L2R tunnel engineering drawing in Fig. 3. The beam is horizontal both entering and leaving the L2R line, but at a height difference of 7.864 m. The full length of the L2R line is 272 m, with a maximum vertical incline of 3.38° and a horizontal bending of $\theta = 68.75^\circ$ (Fig. 3).

The L2R lattice is based on a quadrupole-doublet cell structure taken from the ESS High Energy Beam Transport (HEBT) line design. The cell length is 8.52 m long, each quadrupole is 0.35 m long and the separation of the mid-points of the quadrupoles in each doublet is 1.08 m. The remaining part of the cell constitutes a drift space which is 7.09 m long. It is in this long drift where the dipole magnets are placed for the transfer line.

In designing the lattice, it is important to keep below the ESS beam-loss limit of 1 W/m [7] which restricts the radioactive activation of the accelerator elements. To this end, the dipole strengths are set at 0.15 T, which limits H^- losses from Lorentz stripping to a fractional loss of $5.7 \times 10^{-8}/m$ [8], corresponding to a stripping loss in the dipole magnets of 0.3 W/m for a 5 MW beam. The 0.15 T field corresponds to a dipole bending radius of 73.5 m, which is used for all horizontal and vertical dipole magnets in the transfer line. All dipole magnets in the L2R line have been taken to be sector dipoles.

Beam dynamics simulations have been performed in TraceWin [9] from the start of the Drift Tube Linac (DTL) to the end of the L2R transfer line. The L2R quadrupole strengths are optimised to make the L2R line achromatic (that is, with no output horizontal and vertical dispersion) and to limit intra-beam stripping by avoiding beam sizes that are too small. A matched beam is also ensured between accelerator sectors by matching the Twiss parameters sector-to-sector.

The optimised choice of phase advance is shown in Fig. 4. The phase advance up to and including the HBL matches closely that used for protons, to allow concurrent operation of protons and H^- ions. There is no step in the transverse phase advance on entering the L2R line to ensure efficient matching; beam matching is performed in TraceWin using the last 2 cells in the HBL section and the phase advance adjustment is minimal as shown in Fig. 4.

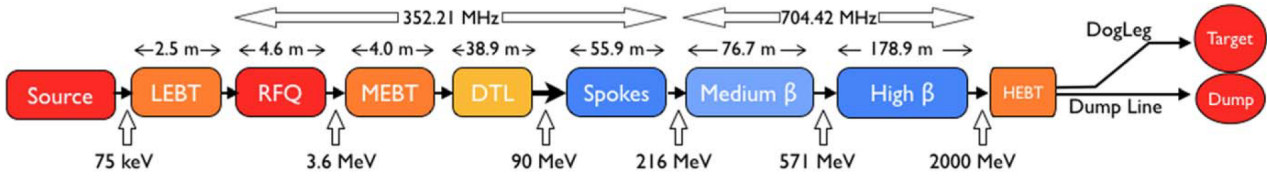


Figure 2: Overview of the ESS layout [4].

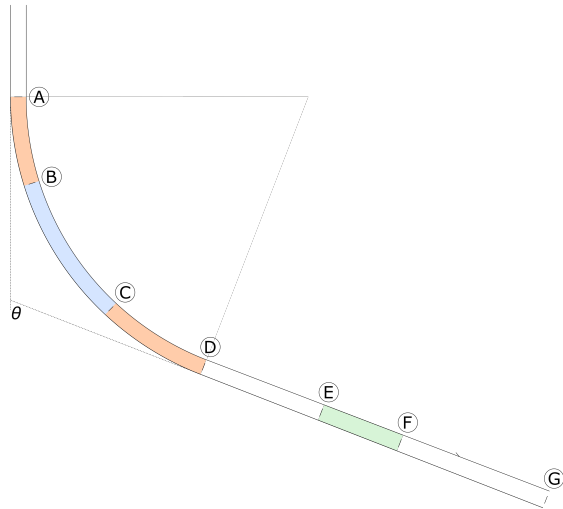


Figure 3: Layout of the L2R transfer line [6], showing horizontally bending sections A–B and C–D in orange, combined horizontally and vertically down-bending section B–C in blue and vertically up-bending section E–F in green.

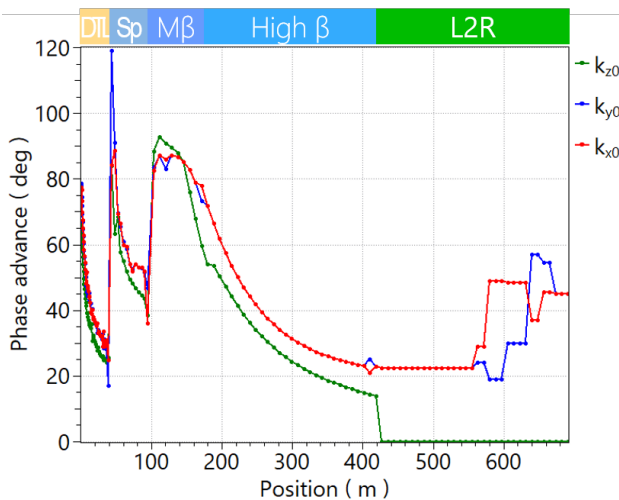


Figure 4: Transverse x (red), transverse y (blue) and longitudinal (green) phase advance per cell along the linac and L2R line. Positions are given relative to the start of the DTL. The lattice sections are indicated along the top of the plot.

In order to make the L2R line achromatic, the total phase advance is set to a multiple of 180° [10]. A relatively low transverse phase advance of $22.5^\circ/\text{cell}$ is used at the beginning of the L2R line, providing relatively weak transverse

beam focusing [11] and a large transverse beam size of up to ± 4 mm (root mean square) in the dispersive section. Critically, this large beam size limits the intra-beam stripping losses [12] to under 0.4 W/m, at or below the level observed in the linac (Fig. 5).

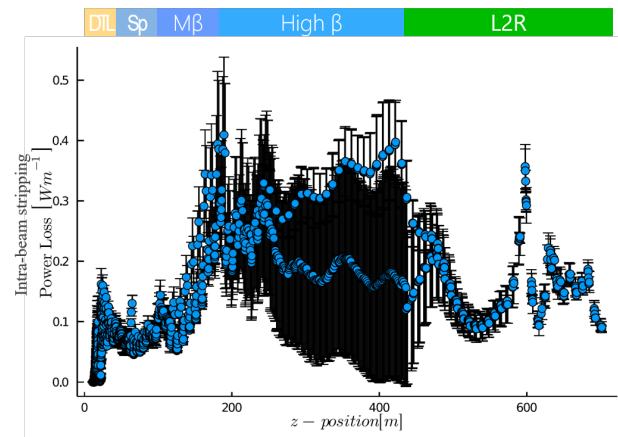


Figure 5: Intra-beam stripping power loss along the linac and L2R line. Positions are given relative to the start of the DTL. The lattice sections are indicated along the top of the plot.

The significance of intra-beam stripping losses decrease along the L2R line as the longitudinal bunch length increases in the absence of accelerating cavities for longitudinal focusing. Therefore, we take the opportunity to ramp up the phase advance from $22.5^\circ/\text{cell}$ to $45^\circ/\text{cell}$ (Fig. 4), increasing the transverse focusing and reducing the transverse beam size to below ± 2 mm (root mean square). This has the benefit that the number of cells with vertically up-bending dipole magnets (section E–F in Fig. 3) can be reduced from 8 to 4, reducing the number of magnets required for the project, whilst keeping the 180° requirement to keep the line achromatic.

ERROR STUDY

Beam losses are expected from accelerator-element misalignment, as well as magnet-strength errors, and accelerator cavity (field amplitude and phase) errors. The effect of these errors on the H^- beam has been simulated in TraceWin, assuming the nominal ESS accelerator element tolerances [4] and while operating a pulse-to-pulse orbit correction. The study is comprised of a single-lattice simulation from the DTL to the end of the transfer line.

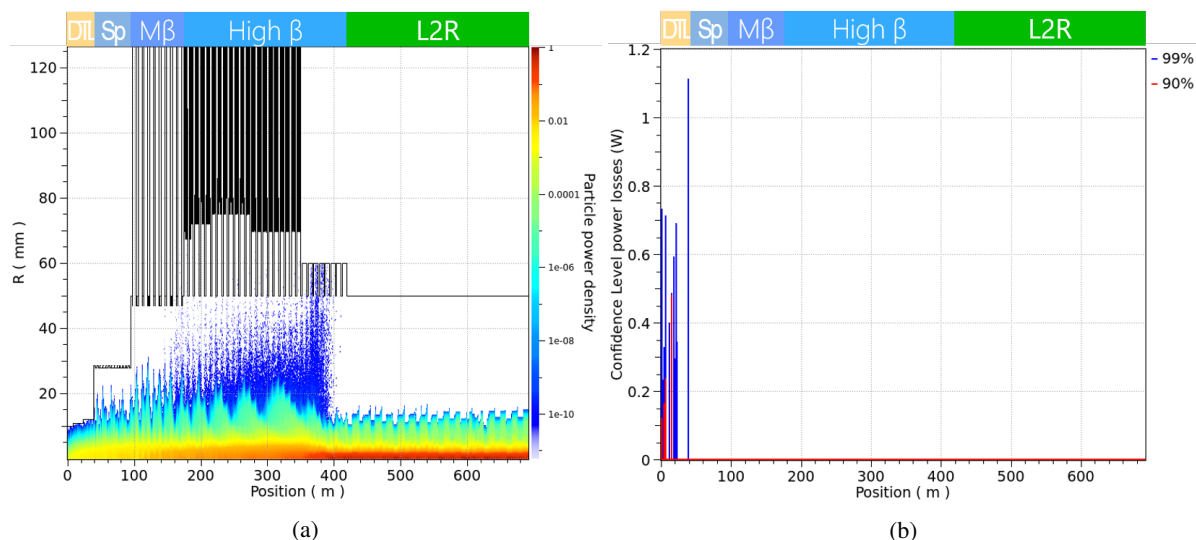


Figure 6: (a) Particle power density and (b) 99% (blue) and 90% (red) confidence levels for power losses for 1000 simulated machines with static and dynamic errors. Positions are given relative to the start of the DTL. The lattice sections are indicated along the top of the plots.

The simulation works by first applying the static errors and then tracking a beam in single particle mode. The corrector-to-BPM feedback loops perform an orbit correction on a pulse-to-pulse basis, adjusting for these static errors. Finally, the dynamic errors are applied to a machine containing static errors with the corrections applied [4], and the beam is tracked through the machine using 200,000 macro particles. For the results presented here, 1000 machines are simulated, each with a random set of errors conforming to the error distributions defined above.

The particle power density along the accelerator line is shown in Fig. 6(a). Most losses are recorded along the 39 meter DTL, where the beam aperture is most restrictive. The corresponding power loss, in Fig. 6(b), shows that the losses are kept below the 1 W per element level, at a 99% confidence level. Note that the outermost halo in Fig. 6(a) represents a particle power density of less than a billionth of the fully accelerated beam core; this halo represents a beam power in the milliwatt range and, therefore, is not problematic even if lost. Note that the H^- stripping losses, such as Lorentz magnetic stripping and intra-beam stripping, discussed above are to be added to the results of the error studies presented in Fig. 6.

CONCLUSIONS

The study for an upgrade of the ESS linac to produce a 2.5 GeV, 5 MW H^- beam has been presented, together with the design of an achromatic L2R transfer line to take the beam to an underground accumulator ring. The design has been validated by start-to-end simulations from the DTL in the linac to the end of the L2R line.

Particle losses have been addressed to keep the total loss below the 1 W/m limit. In particular, the Lorentz stripping is kept at 0.3 W/m in the dipole magnets and the intra-beam

stripping losses are maintained below 0.4 W/m by a careful control of the beam phase advance and the associated beam size. Losses due to static and dynamic errors have been confirmed to be below the 1 W per element level and are concentrated in the DTL where the beam aperture is most restrictive.

ACKNOWLEDGEMENTS

ESSnuSB has received funding from the European Union's Horizon 2020 research and innovation programme under grant agreement No 777419.

REFERENCES

- [1] ESSnuSB, <https://essnusb.eu/>.
- [2] M. Dracos, "The European Spallation Source Neutrino Super Beam Design Study", *J. Phys. Conf. Ser.*, vol. 1067, p. 042001, 2018. doi:10.1088/1742-6596/1067/4/042001
- [3] European Spallation Source, <https://ess.eu>
- [4] R. Garoby *et al.*, "The European Spallation Source Design", *Phys. Scr.*, vol. 93, p. 014001, Dec. 2017. doi:10.1088/1402-4896/aa9bff
- [5] E. Baussan *et al.*, "A very intense neutrino super beam experiment for leptonic CP violation discovery based on the European spallation source linac", *Nucl. Phys. B*, vol. 885, pp. 127–149, 2014. doi:10.1016/j.nuclphysb.2014.05.016
- [6] R. Johansson, "ESSnuSB project layout drawing", ESS Drawing Number ESS-1165084.2.
- [7] L. Tchelidze, "Input criteria for shielding calculations and hands on maintenance conditions for ESS accelerator", ESS Rep. ESS-0008351, 2019.
- [8] P. B. Keating *et al.*, "Electric-field-induced electron detachment of 800-MeV H^- ions", *Phys. Rev. A*, vol. 52, p. 4547, 1995. doi:10.1103/PhysRevA.52.4547

- [9] D. Uriot and N. Pichoff, *TraceWin manual*, Gif-sur-Yvette, Paris, France, Jun. 2021, pp. 1-216; <http://irfu.cea.fr/dacm/logiciels/codesdacm/tracewin/tracewin.pdf> Spain, 2011.
doi:10.5170/CERN-2013-001.171
- [10] T. Satogata, “More Lattice Optics and Insertions”, presented at *US Particle Accelerator School*, Stony Brook University, Melville, NY, USA, 2011.
- [11] B. Holzer, “Beam optics and lattice design for particle accelerators”, presented at *CERN Accelerator School*, Bilbao, Spain, 2016.
- [12] T. Maruta, “Power Upgrade Plan of J-PARC Linac and Loss Estimation”, presented at *Workshop on Upgrading Existing High Power Proton Linacs*, Lund, Sweden, 2016.